Preliminary communication / communication

Isomorphous substitution in zeolites

Rosario Aiello [a,*], Janos B. Nagy [b], Girolamo Giordano [a],
Andrea Katovic [a], Flaviano Testa [a]

[a] *Dipartimento di Ingegneria chimica e dei materiali, Università della Calabria, Via Pietro Bucci, 87030 Rende, CS, Italy*
[b] *Laboratoire de RMN, facultés universitaires Notre-Dame-de-la-Paix, 5000 Namur, Belgium*

Abstract

This chapter deals with the isomorphous substitution in the zeolitic framework. Some specific cases among the research works of the authors have been selected. B-MFI, Fe-MFI, Fe-BEA and Fe-MOR zeolites have been examined optimizing the synthesis parameters. B-MFI zeolite has been synthesized in fluoride media, while the other zeolites have been prepared in alkaline media. In all cases isomorphous substitution in the zeolitic structure, even if not complete, is obtained. It should be pointed out that in fluoride media and in presence of K^+ and Cs^+ ions more than four boron atoms per unit cell can be incorporated in the MFI structure. *To cite this article: R. Aiello et al., C. R. Chimie 8 (2005)*.

Résumé

Cet article traite de la substitution isomorphe dans la charpente zéolitique. Des cas spécifiques ont été choisis parmi les travaux de recherche des auteurs. Ainsi, les B-MFI, Fe-MFI, Fe-BEA, et Fe-MOR sont examinés du point de vue de leurs paramètres de synthèse. B-MFI a été synthétisé en utilisant la voie fluorure, tandis que les trois autres zéolithes ont été synthétisées en milieu alcalin. Dans tous les cas, la substitution isomorphe a eu lieu, même si elle n'est pas complète, dans la structure zéolitique. Il faut souligner qu'en milieu fluorure et en présence d'ions K^+ ou Cs^+, plus de 4 atomes de bore peuvent être introduits par maille dans la structure de MFI. *Pour citer cet article : R. Aiello et al., C. R. Chimie 8 (2005)*.

* Corresponding author.

E-mail address: r.aiello@unical.it (R. Aiello).

1. Introduction

The isomorphous substitution of Si by other tetrahedrally coordinated heteroatoms such as B^{III} [1,2] Al^{III} (ZSM-5) [3] Ti^{IV} (TS-1) [4–9], Ga^{III} [10–14] and Fe^{III} [15–18] in small amounts (up to 2–3 wt.%) provides new materials showing specific catalytic properties in oxidation and hydroxylation reactions related to the coordination state of the heteroatom [19]. Moreover, MFI-type materials with trivalent metal present in tetrahedral (T) sites have had a tremendous impact as new shape-selective industrial catalysts having tunable acidic strength. In fact, the acidic strength of the protons in the bridged $Si(OH)M^{III}$ (M = B, Al, Fe, Ga) groups depends on the nature of the trivalent heteroatom. Indeed, the choice of M^{III} critically affects this acidic property according to the sequence Al > Fe = Ga >> B [20–23]. In this paper, we shall emphasize the preparation of B-MFI, Fe-MFI, Fe-BEA and Fe-MOR. All the reported results stem from our research work.

The B-MFI is synthesized in fluoride medium, because, as we shall see, even in presence of tetrapropylammonium bromide (TPABr) more than four B can be introduced per unit cell into the MFI framework. In alkaline media, this can only be achieved if ethylenediamine is used instead of TPABr [24]. On the other hand, we also show, that the alkaline media is also convenient for the isomorphous substitution, provided that appropriate complexing agents are chosen to stabilize the metal ions to be introduced into the zeolitic structure.

2. Results and discussion

2.1. Synthesis of B-MFI using the fluoride route [25]

Borosilicalites of MFI structure were obtained with all the different cations used and over the whole range of concentrations. Table 1 shows the physicochemical characterization data and Table 2 the ^{11}B-NMR data for the different borosilicalite samples obtained with different amounts of H_3BO_3 and different alkali cations. Fig. 1 shows typical ^{11}B-NMR spectra of a precursor and the corresponding calcined samples. The framework tetrahedral boron (T) is characterized by a chemical shift of ca. –3.9 ppm with respect to BF_3–

Table 1

Physicochemical characterization of precursor samples of borosilicalites synthesized from 9 MF–x H_3BO_3–10 SiO_2–1.25 TPABr–330 H_2O at 170 °C

x	M	B/u.c. [a]	M/u.c. [b]	TPA/u.c. [c]
0.1	NH₄	0.8	–	3.8
	Na	1.2	0.5	3.7
	K	1.0	0.7	3.4
	Cs	1.2	0.1	3.8
10	NH₄	4.4	–	3.5
	Na	6.3	2.0	3.7
	K	8.4	3.2	2.8
	Cs	9.4	3.7	2.4

[a] NMR values.
[b] Atomic absorption values.
[c] Thermal analysis values.

OEt_2 [26]. In the presence of Cs and 10 mols of H_3BO_3 in the initial gel, up to 9.4 tetrahedral B/u.c. can be incorporated in the structure.

However, during the calcination a large amount of boron is eliminated from the structure (Table 2) and the relative amount of boron in the tetrahedral configuration decreases. The extra-framework boron is in a tetrahedral configuration in most of the cases, characterized by chemical shift of –2.0 ppm. Sometimes, some of the extra-framework boron can also take a trigonal configuration, as in the various borates. In this case, the broad NMR line is situated between 5.5 and 27 ppm. The quantitative determination of the trigonal boron was made by considering an average value of the quadrupole coupling constant of ca. 2.5 MHz [27] and using the corrections for the line intensities depending on the value of $v_Q^2/v_L \cdot v_{rot}$ with v_Q = 1.25 MHz, v_L = 128.3 MHz and v_{rot} = 9 kHz [28,29]. The measured intensities were corrected by a factor of 1/0.33 = 3. No correction was made for the intensities of the lines of the tetrahedral boron (Q_{cc} = 0.2 MHz [27]). The total amount of TPA/u.c. is equal to 3.4–3.8 for samples synthesized with 0.1 mols of H_3BO_3. For the K- and Cs-borosilicalite samples, the amount of TPA/u.c. decreases to 3.2 and 2.7 for samples synthesizes with 4 mols of H_3BO_3 and to 2.8 and 2.4 for samples obtained with 10 mols of H_3BO_3. The decrease in TPA/u.c. is also indicative of boron incorporation into the MFI structure. Indeed, it was previously observed that the increase in Al in the zeolitic framework was accompanied by a decrease in TPA/u.c. [30]. The M/u.c. remains quite low for low B-containing samples (Table 1). It varies from 0.1 to 0.7. As more

Table 2
^{11}B-NMR data of borosilicalites synthesized from $9MF–xH_3BO_3–10SiO_2–1.25TPABr–330H_2O$ at 170 °C

x	M	Sample [a]	δ (ppm)	I (%)	B_{tet}/u.c. [b]	δ (ppm)	I (%)	B trigonal	
								δ (ppm)	I (%)
0.1	NH$_4$	pr	−4.2	100	0.8				
		c	−4.0	27	0.2	−2.9	18	5.6–17	55
	Na	pr	−4.1	100	1.2				
		c	−3.7	20	0.4	−2.9	22	5.2–17	45
	K	pr	−4.2	100	1.0				
		c	−3.7	63	0.5	−2.9	37		
	Cs	pr	−3.3	100	1.2	−			
		c	−4.0	12	0.24	−2.9	47	5.2–17	34
10	NH$_4$	pr	−4.1	80	3.5	−2.9			
		c	−			−			
	Na	pr	−4.0	73	4.6	−2.9	22	5.5–17	5
		c	−3.6	53	3.3	−2.9	6	5.5–17	41
	K	pr	−3.9	70	5.9	−2.9	30		
		c	−3.9	17	1.0	−2.9	34	1–17	49
	Cs	pr	−3.9	32	2.9	−2.9	68	5.5–17	11
		c	−3.8	54	5.1	−2.8	26	5.5–17	20

[a] pr: precursor; c: calcined.
[b] Corresponding to the amount of boron at ca. −4 ppm.

boron is incorporated into the structure, this amount increases to 3.7 for the Cs-borosilicalite. If boron is incorporated into the zeolitic framework, its presence leads to a contraction of the unit cell because the atomic radius of the B atom (0.98 Å) is smaller than that of silicon atom (1.17 Å). The cell parameters and the unit cell volume decrease monotonously as a function of B/u.c. [31]. The decrease is largest for the K- and Cs-borosilicalites. From a correlation between the unit cell volume and B/u.c. reported in Ref. [32], it can be predicted that some five to six boron atoms can be incorporated into the MFI structure using K$^+$ ions. As was already mentioned above, Cs$^+$ at high H$_3$BO$_3$ concentrations behaves quite peculiarly. For example, the B/u.c. in the framework increases during calcination with $x = 10$ mols (Table 2 and Fig. 2).

During calcinations, carried out at 500 °C in a flow air, the NMR line at −3.9 ppm increases, while the one at −2.0 ppm decreases. There is also some increase in the 5.5–17 ppm line. It seems as if the −2.0 ppm line which was attributed to extraframework tetrahedral boron is transformed predominantly to the −3.9 ppm line, i.e. the boron in the structure in tetrahedral configuration, and partially to non-framework trigonal boron at 5.5–17 ppm. Hence we have to modify the attribution of the −2.0 ppm line. It is possible that the "extraframework" tetrahedral boron in the precursor is really not an extraframework boron,
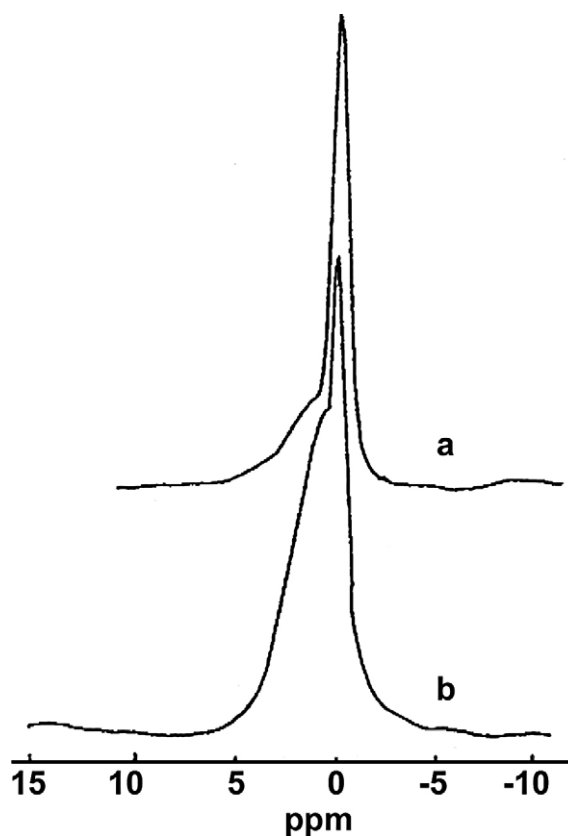
Fig. 1. MAS ^{11}B-NMR spectra of (**a**) K-borosilicalite precursor and (**b**) calcined samples obtained with 10 mol of H$_3$BO$_3$.
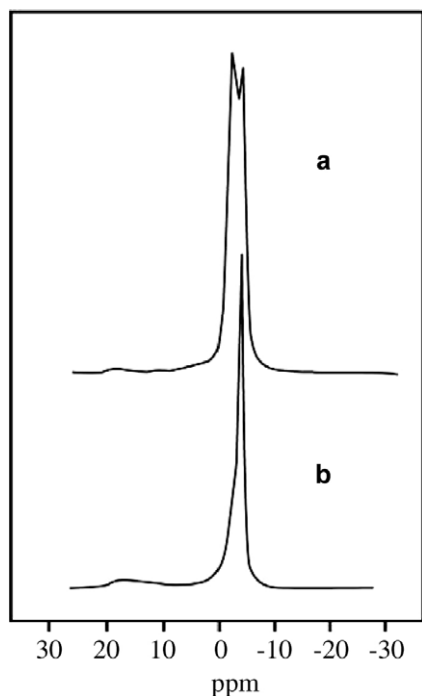
Fig. 2. MAS ^{11}B-NMR spectra of precursor (**a**) and calcined (**b**) Cs-borosilicates synthesized with 10 mol of H_3BO_3.

but characterizes a tetrahedral boron which is still partially linked to the structure. If this is the case, a rather high amount of SiOH defect groups should be present in these samples. This is confirmed by the ^{29}Si-NMR spectra, where indeed a high concentration of SiOX group at –103 ppm is detected (Fig. 3). Interestingly,
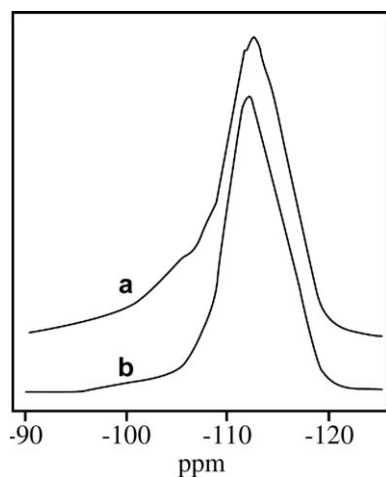

Fig. 3. MAS ^{29}Si-NMR spectra of (a) precursor and (b) calcined Cs-borosilicates synthesized with 10 mol of H_3BO_3.

the K-borosilicate samples do not show any anomaly (Table 2 and Fig. 1). No SiOX defect groups were detected in the precursor samples at high boron concentration.

The attribution of the –2.0 ppm line in the ^{11}B-NMR spectra to partially deformed framework tetrahedral boron such as $[(SiO)_3BOH]^-$ (i.e. having non-bridging oxygen in the structure) was also suggested for reedmergnerite [27]. From this study it can be concluded that greater than four B/u.c. can be introduced into silicalite-1 using a fluoride-containing medium in the presence of either K^+ or Cs^+ ions. We can see now that the maximum of four B/u.c. observed in previous studies carried out in both alkaline [33] and fluoride [34] media is essentially linked to Na^+, which was the inorganic cation used. Indeed it was shown [33] that Na^+ preferentially accompanied Al in the structure, while TPA^+ is the preferential cation to $[SiOB]^-$ negative charges. It was also demonstrated that the boron species incorporated into the zeolite structure were in a trigonal form, i.e. $B(OH)_3$ in the alkaline medium. As only a maximum of 4/u.c. of TPA^+ can be included in the channel, the maximum B/u.c. also equals four. The preferential interaction between $[SiOAl]^-$ and Na^+ on the one hand between $[SiOB]^-$ and TPA^+ on the other can be understood on the basis of the hard and soft acid–base interaction. It is well known that hard acids accompany better hard bases and soft acids link preferentially to soft bases: as Na^+ is a harder acid than TPA^+, $[SiOAl]^-$ is also a harder base than $[SiOB]^-$. The preferential interactions lead then to the TPA^+–$[SiOB]^-$ pairs, as was demonstrated previously [33]. If, however, the Na^+ ions are replaced by either K^+ or Cs^+, which are softer acids than Na^+, the presence of these ions could also favor the introduction of boron into the zeolite structure, as preferential $[SiOB]^-$ K^+ or $[SiOB]^-$ Cs^+ pairs can be formed. The presence of either K^+ or Cs^+ in the channels lowers the possibility of introducing four TPA/u.c. Indeed, it is found for samples having more, than four B/u.c. that TPA/u.c. decreases. The thus-created available free space can then be occupied by the other "soft" counteractions (K^+ or Cs^+) and no defect groups have to be created in the structure. Hence K^+ or Cs^+ show preferential interaction with $[SiOB]^-$ charges as Na^+ does with $[SiOAl]^-$. In the latter case, it is possible to introduce up to 8–10 Al/u.c. [30,33]. Hence, in the presence of K^+ or Cs^+ greater than four B/u.c. can be obtained.

2.2. Fe-MFI synthesized by the alkaline route [35]

Fe-MFI products were obtained in alkaline media using either oxalic or phosphoric acid as complexing agents. In addition, the initial gels were prepared either without ethylene glycol (system A) or in the presence of ethylene glycol (system B) (Table 3).

The general compositions of the gels were: x Na$_2$O–y TPABr–z Al$_2$O$_3$–SiO$_2$–q Fe$_2$O$_3$/p HA–20 H$_2$O where $x = 0.1$–0.32; $y = 0.02$–0.08; $z = 0$–0.05; $q = 0.005$–0.025; the ratio $p/q = 3$ and HA stands for H$_2$C$_2$O$_4$ or H$_3$PO$_4$. The second system was prepared from the following initial reaction mixture: 0.16 Na$_2$O–x TPABr–y EG–z Al$_2$O$_3$–SiO$_2$–q Fe$_2$O$_3$–p HA–10 H$_2$O where $x = 0.08$; $y = 0$–6.0; $z = 0$–0.05; $q = 0.005$–0.1; the ratio $p/q = 3$ and HA stands for H$_2$C$_2$O$_4$ or H$_3$PO$_4$ and EG for ethylene glycol.

First of all it can be observed that if only TPABr is present in the initial gel (system A), Fe-MFI zeolite can be obtained in a large Si/Fe range and a reaction time of 1–4 days (samples 1(A)–7(A) in Table 3). The so obtained Fe-MFI products are thermodynamically stable. Indeed, if the reaction time is increased, the transformation of the MFI structure into more stable phases is not observed. Even after a thermal treatment up to 850 °C, the MFI is the sole phase detected. The crystallization time increases with increasing iron and/or aluminum content of the starting hydrogel (compare samples 1(A) and 2(A), and samples 4(A) and 6(A), respectively).

In system B, the formation of Al-MFI is very easy in the presence of ethylene glycol (EG) only (sample 21(B)). This result confirms the data reported in Ref. [36]. In the presence of EG, only Al rich hydrogels were studied, because no pure MFI zeolite could be synthesized in silica rich system [34]. The presence of EG is also able to direct the formation of MFI structure in the presence of both Al and Fe (samples 22(B) and 23(B)). If TPABr is also present in the initial gel, the reaction time decreases (see samples 11(B) and 18(B), and 12(B) and 19(B)). In addition, the stability of the final MFI products also increases with increasing TPABr content of the gel. Indeed, pure Fe-MFI sample is obtained with 0.08 TPABr (sample 8(B)) even after 6 days of crystallization, while sample 14(B) synthesized in the presence of 0.02 TPABr shows the co-crystallization of MFI with quartz and cristobalite after 4 days of crystallization. The increasing TPABr content in the initial hydrogel results in decreasing reaction time (see samples 14(B) and 8(B)). On the other hand, the increase in the

Table 3
The MFI synthesized products varying the composition of the starting hydrogel in the type A and B systems

Sample	Si/Fe$_{gel}$	Si/Al$_{gel}$	TPABr	EG	Time (days)	Product	Si/Al$_{cryst}$	Si/Fe$_{cryst}$
1(A)	100	∞	0.08	0.0	1	MFI	–	85.5
2(A)	10	∞	0.08	0.0	3	MFI	–	15.4
3(A)	100	100	0.08	0.0	1	MFI	97.7	73.8
4(A)	10	∞	0.02	0.0	3	MFI	–	–
6(A)	10	10	0.02	0.0	4	MFI	25.0	307
7(A)	∞	25	0.02	0.0	2	MFI	16.5	–
8(B)	20	∞	0.08	3	1	MFI	–	258
9(B)	6.67	∞	0.04	3	2	MFI	–	252
10(B)	6.67	∞	0.04	3	5	MFI	–	–
11(B)	20	10	0.04	3	2	MFI	23.5	418
12(B)	10	10	0.04	3	2	MFI	23.0	459
13(B)	6.67	10	0.04	3	6	MFI	24.1	442
14(B)	20	∞	0.02	3	2	MFI	–	504
17(B)	20	20	0.02	3	2	MFI	–	–
18(B)	20	10	0.02	3	5	MFI	–	–
19(B)	10	10	0.02	3	5	MFI	29.1	403
21(B)	∞	20	0.0	3	3	MFI	13.7	–
22(B)	20	20	0.0	3	2	MFI	35.0	423
23(B)	20	10	0.0	3	5	MFI	18.1	369

EG: ethylene glycol; A: without EG; B: with EG.

initial Al or Fe-content in the hydrogels leads to the increase in reaction time: compare samples 9(B) and 13(B) for the Al-content and samples 11(B) and 13(B) for the influence of Fe-content.

For both systems the pH value plays an important role in the crystallization process. As a matter of fact, pure MFI zeolite is formed when the pH value of the initial hydrogel is between 9 and 12.5.

The chemical analyses data are also reported in Table 3 for both systems A and B. It can be noticed that for type A synthesis system the amount of iron incorporated into the zeolitic structure is related to its content in the TPABr rich hydrogels (see samples 1(A) and 2(A)). For these TPABr rich hydrogels, when both iron and aluminum are present (sample 3(A)), iron is incorporated preferentially with respect to aluminum. However, if the TPABr content decreases to 0.02, iron cannot be incorporated as efficiently (sample 6(A)) and aluminum is preferentially incorporated.

This behavior can be explained by the different interaction between soft and hard acids with iron and aluminum atoms. It is known that hard acids accompany better hard bases and soft acids prefer the soft bases. As Na^+ is a harder acid than the TPA^+ they interact well, respectively, with $[Si–O–Al]^-$ and $[Si–O–Fe]^-$ groups, since $[Si–O–Al]^-$ is a harder base than the $[Si–O–Fe]^-$. This kind of interactions has been demonstrated by different authors in the case of B-MFI-type zeolite (see above). In the case of system-type B (with EG) we detect always a low amount of iron in the MFI samples, even in the presence of a high TPABr content (see sample 8(B), Table 3). Oppositely, the amount of aluminum in the zeolitic framework is related to its content in the starting hydrogel and it is almost always a high amount. This confirms that the hydrogel systems that contain both sodium and alcohol, such as EG, show a high amount of sodium in the crystals [37,38] and consequently they prefer the interaction with the $[Si–O–Al]^-$ groups and favor the Al incorporation. Probably the EG molecules compete with the TPA^+ cations and they fill the zeolitic channels as detected by thermal analysis, in fact we found the EG molecules intact in the MFI channels.

The size of the crystals obtained from system A decreases when the amount of iron incorporated in the zeolite increases, and it changes from 10 µm (samples 1(A), Table 3) to 2.3 µm (sample 2(A), Table 3). Also the morphology for the samples changes from brick-like to spheres (see Figs. 4 and 5).
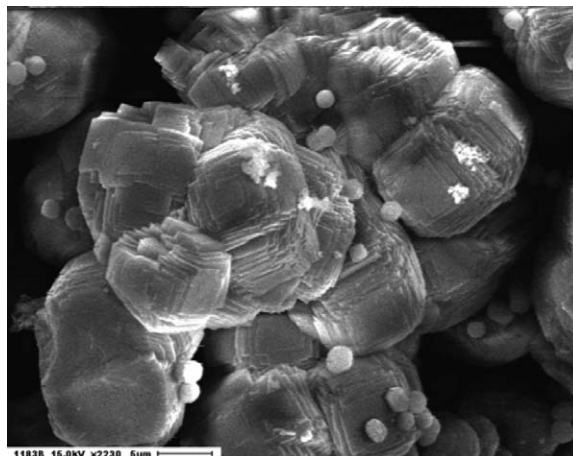

Fig. 4. Scanning electron micrograph of Fe-MFI sample 1(A).

These observations give an indirect confirmation of the iron incorporation into the MFI framework. The presence of aluminum in the zeolite allows a reduction in crystal size compared to that of the Al-free samples. In fact, sample 3(A) shows a spherical habitus with a diameter of 5 µm, whereas sample 2(A) evidences the same morphology with a smaller size (2.7 µm) due to the high amount of aluminum and iron incorporated into the zeolitic framework. The morphology of the samples obtained from the system B shows a brick-like shape for both iron and iron–aluminum systems. Also in this case the crystal size decreases when the amount of Al incorporated into the zeolite increases and changes from 12 to 1 µm.
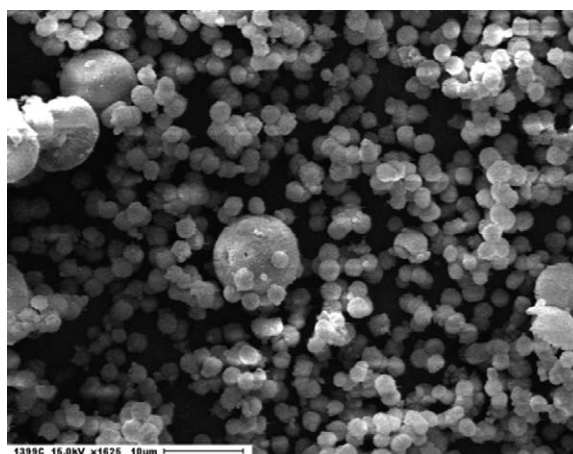

Fig. 5. Scanning electron micrograph of Fe-MFI sample 2(A).

2.3. Synthesis of Fe-BEA using the alkaline route [39]

Using the reagents proposed for the synthesis of Fe-BEA in Ref. [40] no Fe-BEA zeolite could be reproduced. Indeed, starting from a gel of composition of 40 SiO_2–1.02 $Fe(NO_3)_3 \cdot 9 \ H_2O$–19.04 TEAOH–4 NaOH–676 H_2O and using a 24-h ageing time only amorphous phase was obtained at 120 °C after 12 days. Similar unsuccessful tentative was made if the ageing was done at 298 °C for 3 h. The reaction temperature of 150 °C did not lead to any Fe-BEA zeolite. Finally, even if TEAOH 25% in methanol solution was used no Fe-BEA zeolite could be obtained following the method proposed in Ref. [41]. In order to find a well reproducible method using our reagents, we have systematically varied the amount of iron source, the amount of TEAOH, the ageing time of the gel, the reaction time and the temperature of the reaction. The general composition of the gel was the following: 40 SiO_2–x $Fe(NO_3)_3 \cdot 9 \ H_2O$–$y$ TEAOH–4 NaOH–676 H_2O with $x = 0.38, 0.49, 0.51$, $y = 19.04$, ageing time = 2, 18, or 24 h, reaction time = 7, 9, 10, 20, 21, 22, 26, 28, or 30 days. Only one synthesis led to Fe-Beta, with $x = 0.49$, $y = 19.04$, 24-h ageing and 20 days of synthesis time at 120 °C. Even this synthesis was not reproducible. Note that using fumed silica instead of TEOS as silica source, some unidentified layered compounds were obtained. For $x = 0.45, 0.49$ and 0.60 and $y = 10.88, 13.6$ and 16.3, ageing time = 2 or 24 h, reaction time = 16, 18, 20, 21, 22, 25, 29 or 40 days, $T = 120$ °C, Fe-BEA co-crystallize in most of the cases with an unknown phase having a diffraction peak at 5.6 2θ. Note that a similar peak was obtained during the synthesis of a low Al content Beta zeolite [42]. This peak disappears during calcinations at 450 °C. As the reaction temperature of 120 °C was not adequate to obtain pure Fe-BEA in a reproducible way, the reaction temperature was raised to 150 °C. At this temperature the amounts of $Fe(NO_3)_3 \cdot 9 \ H_2O$ and TEAOH are also varied in order to optimize the synthesis conditions. The data are reported in Table 4.

It is clearly seen from Table 4 that, in particular conditions, pure Fe-BEA can be obtained in a reproducible manner at 150 °C. The conditions are 0.45 or 0.60 $Fe(NO_3)_3 \cdot 9 \ H_2O$, 13.6 or 16.3 TEAOH, 24 h ageing time and reaction time 4–8 days. The narrow crystallization fields are reported in Fig. 6, where the crystallization field of Fe-BEA is surrounded at higher

Table 4

Synthesis conditions for the Fe-BEA obtained from gels of composition 40 SiO_2–x $Fe(NO_3)_3 \cdot 9 \ H_2O$–$y$ TEAOH–4 NaOH–676 H_2O at 150 °C[a]

Sample	x	y	Reaction time (days)	Product
BEA-1	0.60	16.3	4–8	Fe-BEA
BEA-2	0.45	16.3	8	Fe-BEA
BEA-3	0.45	13.6	8	Fe-BEA

[a] Ageing time: 24 h.
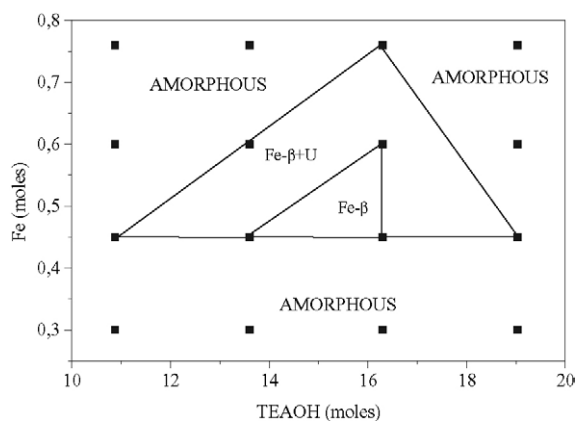
Fig. 6. Crystallization fields of Fe-BEA zeolite from gels of composition 40 SiO_2–x $Fe(NO_3)_3 \cdot 9 \ H_2O$–$y$ TEAOH–4 NaOH–676 H_2O at 150 °C.

Fe-content by a phase where Fe-BEA coexists with an unknown phase U. Note that at low ageing time of the gels (2 h), only an amorphous phase was obtained in all cases. The white color of all the final crystalline Fe-BEA zeolite samples suggests that Fe(III) occupies framework tetrahedral sites in the structure. In the zone of crystallization of Fe-BEA – i.e. 0.60 $Fe(NO_3)_3 \cdot 9 \ H_2O$ and 16.3 TEAOH-(Fe, Al)-BEA and Al-BEA were also synthesized maintaining the same moles of iron and aluminum source equal to 6. The data are reported in Table 5. It is seen that only the crystalline phases (Fe, Al)-BEA or Al-BEA were obtained in all synthetic runs

Table 5

Synthesis conditions for (Fe, Al) and Al-BEA obtained from gels of composition 40 SiO_2–x $Fe(NO_3)_3 \cdot 9 \ H_2O$–$y$ $Al(OH)_3$–16.3 TEAOH–4 NaOH–676 H_2O at 150 °C[a]

Sample	x	y	Reaction time (days)	Product
BEA-4	0.30	0.30	4	(Fe, Al)-BEA
BEA-5	0.18	0.42	4–6	(Fe, Al)-BEA
BEA-6	0.06	0.54	3–5	(Fe, Al)-BEA
BEA-7	0	0.60	4–6	Al-BEA

[a] Ageing time: 24 h.

Table 6

Products obtained starting from the hydrogel of composition x Na$_2$O–0.2 TEABr–y Al$_2$O$_3$–z Fe$_2$O$_3$–w C$_2$H$_2$O$_4$–SiO$_2$–20 H$_2$O at 170 °C

Sample	Na$_2$O	Al$_2$O$_3$	Fe$_2$O$_3$	Time (days)	Products	Si/Al$_{zeo}$	Si/Fe$_{zeo}$
MOR-1	0.15	0.02	–	2.5	MOR	24.1	–
MOR-2	0.27	0.02	–	2.5	MOR	–	–
MOR-3	0.15	0.025	–	4	MOR	–	–
MOR-4	0.15	0.02	0.005	5	MOR	24.7	59.1
MOR-5	0.15	0.02	0.010	8	MOR	24.9	37.5
MOR-6	0.17	0.02	0.015	11	MOR	23.9	26.6

already at 3 or 4 days crystallization time. These results reinforce the existence of the zone where pure Fe-BEA zeolite samples could be obtained.

2.4. Synthesis of Fe,Al-MOR [43]

The synthesis of both Fe-BEA and Fe-MOR was also tempted using the alkaline medium. The initial gel compositions were x Na$_2$O–0.2 TEABr–z Fe$_2$O$_3$–w C$_2$H$_2$O$_4$–SiO$_2$–20 H$_2$O, where w/z was equal to 3.

First of all it is important to underline that the attempt to obtain a pure iron form of BEA and MOR type zeolite was unsuccessful because the absence of aluminum in the initial hydrogel does not allow the formation of either Fe-BEA or Fe-MOR at the temperatures of 140 and 170 °C, respectively.

In Table 6 the results on the synthesis of the Al-MOR and Al-Fe-MOR zeolites are shown starting from initial gels of composition x Na$_2$O–0.2 TEABr–y Al$_2$O$_3$–z Fe$_2$O$_3$–w C$_2$H$_2$O$_4$–SiO$_2$–20 H$_2$O at the temperature of 170 °C. As expected, the amount of Al in the starting hydrogel is the crucial parameter during the crystallization process. Indeed, the MOR structure was obtained from the mixtures with a Si/Al ratio lower than 33.3. Alkali content influences the nature of the products. A dense phase (quartz) co-crystallizes together with a zeolitic phase which changes into zeolite BEA when the amount of sodium hydroxide in the starting hydrogel is decreased, and a layered phase appeared in the case when the lowest alkali content was tested. This confirms that a great amount of sodium hydroxide is necessary for the synthesis of MOR type zeolite. In any case for the formation of Al or Fe-Al-MOR zeolite the pH value of the starting hydrogel must be higher than 13. In the presence of only iron, this reaction system leads to the formation of quartz and in presence of aluminum content ranging from 0.005 to 0.015 no crystalline phases were detected even for long reaction times. Since with this hydrogel system it was impossible to

obtain mordenite in the absence of aluminum, we tested the iron incorporation in the system that contains the lowest amount of Al (equal to 0.02). The maximum amount of iron that could be introduced into the zeolite was equal to 0.015 (Si/Fe = 33.3); in the case of higher iron contents in the hydrogel, the system did not evolve towards mordenite formation. The crystallization time was prolonged when iron content in the starting hydrogel was increased. In the system without iron (sample MOR-1) crystallizes in 2.5 days, on the contrary for a higher Si/Fe ratio (equal to 33.3, sample MOR-6) 11 days are required. Only for the highest iron loading it was necessary to increase the amount of sodium hydroxide in order to maintain the pH of the hydrogel higher than 13, the value which was previously found to be essential to obtain pure MOR type zeolite.

References

[1] G. Coudurier, A.J. Auroux, C. Vedrine, R. Farlee, L. Abrams, R.D. Shannon, J. Catal. 108 (1987) 1.

[2] R. Millini, G. Perego, G. Bellussi, Top. Catal. 9 (1999) 13.

[3] G.T. Kokotailo, S.L. Lawton, G.T. Olson, W.M. Meier, Nature 272 (1978) 437.

[4] M. Taramasso, G. Perego, B. Notari, US Patent 4,410,501, 1983.

[5] S. Bordiga, S. Coluccia, C. Lamberti, L. Marchese, A. Zecchina, F. Boscherini, F. Buffa, F. Genoni, G. Leofanti, G. Petrini, G. Vlaic, J. Phys. Chem. 98 (1994) 4125.

[6] G. Tozzola, M.A. Mantegazza, G. Ranghino, G. Petrini, S. Bordiga, G. Ricchiardi, C. Lamberti, R. Zulian, A. Zecchina, J. Catal. 179 (1998) 64.

[7] R. Millini, E. Previde Massara, G. Perego, G. Bellussi, J. Catal. 137 (1992) 497.

[8] G. Ricchiardi, A. Damin, S. Bordiga, C. Lamberti, G. Spanò, F. Rivetti, A. Zecchina, J. Am. Chem. Soc. 123 (2001) 11409.

[9] S. Bordiga, A. Damin, F. Bonino, G. Ricchiardi, C. Lamberti, A. Zecchina, Angew. Chem. Int. Ed. Engl. 41 (2002) 4734.

[10] C.R. Bayense, A.P.R. Kentgens, J.W. de Haan, L.J.M. van de Ven, J.H.C.J. van Hooff, J. Phys. Chem. 96 (1992) 775.

[11] X. Liu, J. Klinowski, J. Phys. Chem. 96 (1992) 3403.

[12] C. Otero Areán, G. Turnes Palomino, F. Geobaldo, A. Zecchina, J. Phys. Chem. 100 (1996) 6678.

[13] C. Lamberti, G. Turnes Palomino, S. Bordiga, A. Zecchina, G. Spanò, C. Otero Areán, Catal. Lett. 63 (1999) 213.

[14] R. Fricke, H. Kosslick, G. Lischke, M. Richter, Chem. Rev. 100 (2000) 2303.

[15] R. Szostak, T.L. Thomas, J. Catal. 100 (1986) 555.

[16] S. Bordiga, R. Buzzoni, F. Geobaldo, C. Lamberti, E. Giamello, A. Zecchina, G. Leofanti, G. Petrini, G. Tozzola, G. Vlaic, J. Catal. 158 (1996) 486.

[17] F. Geobaldo, C. Lamberti, S. Bordiga, A. Zecchina, G. Turnes Palomino, C. Otero Areán, Catal. Lett. 42 (1996) 25.

[18] G. Berlier, G. Spoto, S. Bordiga, G. Ricchiardi, P. Fisicaro, A. Zecchina, I. Rossetti, E. Selli, L. Forni, E. Giamello, C. Lamberti, J. Catal. 208 (2002) 64 [REMOVED HYPER-LINK FIELD].

[19] R. Szostak, Molecular Sieves, Van Nostrand Reinhold, New York, 1989, p. 205.

[20] C.T.-W. Chu, C. Chang, J. Phys. Chem. 89 (1985) 1569.

[21] P. Strodel, K.M. Neyman, H. Knötzinger, N. Rösch, Chem. Phys. Lett. 240 (1995) 547.

[22] M.S. Stave, J.B. Nicholas, J. Phys. Chem. 99 (1995) 15046.

[23] D.J. Parrillo, C. Lee, R.J. Gorte, D. White, W.E. Farneth, J. Phys. Chem. 99 (1995) 8745.

[24] G. Perego, G. Bellussi, R. Villini, A. Alberti, S. Zanardi, Micropor. Mesopor. Mater. 58 (2003) 213.

[25] F. Testa, R. Chiappetta, F. Crea, R. Aiello, A. Fonseca, J.B. Nagy, Colloid Surf. A 115 (1996) 223.

[26] Z. Gabelica, J.B. Nagy, P. Bodart, G. Debras, Chem. Lett. (Jpn.) 13 (1984) 1059.

[27] G.L. Turner, K.A. Smith, R.J. Kirkpatrick, E. Oldfield, J. Magn. Reson. 67 (1986) 544.

[28] D. Massiot, C. Bessada, J.-P. Coutures, F. Taulelle, J. Magn. Reson. 90 (1990) 231.

[29] M. Hunger, G. Engelhardt, H. Koller, J. Weitkamp, Solid-State Nucl. Magn. Reson. 2 (1993) 111.

[30] G. Debras, A. Gorge, J.B. Nagy, G. de Clippeleir, Zeolites 5 (1985) 377.

[31] F. Testa, R. Chiappetta, F. Crea, R. Aiello, A. Fonseca, J.B. Nagy, Stud. Surf. Sci. Catal. 94 (1995) 349.

[32] A. Cichocki, W. Lasocha, M. Michalik, Z. Sawlowicz, M. Bus, Zeolites 10 (1990) 583.

[33] R. de Rutier, J.C. Jansen, H. van Bekkum, Zeolites 12 (1992) 56.

[34] M. Soulard, S. Bilger, H. Kessler, J.L. Guth, Zeolites 7 (1987) 463.

[35] G. Giordano, A. Katovic, Stud. Surf. Sci. Catal. 140 (2001) 297.

[36] A. Cichocki, W. Lasocha, M. Michalik, Z. Sawlowicz, M. Bus, Zeolites 10 (1990) 583.

[37] G. Giordano, F. Di Renzo, F. Remoué, F. Famula, D. Plee, P. Schultz, Stud. Surf. Sci. Catal. 142 (2002) 469.

[38] R. De Ruiter, J.C. Jansen, H. Van Bekkum, Zeolites 12 (1992) 56.

[39] D. Aloi, F. Testa, L. Pasqua, R. Aiello, J.B. Nagy, Stud. Surf. Sci. Catal. 87 (1994) 141.

[40] R. Kumar, A. Thangaraj, R.N. Bhat, P. Ratnasmy, Zeolites 10 (1990) 85.

[41] R.B. Borade, A. Clearfield, Micropor. Mater. 2 (1994) 167.

[42] P.R. Hari Prasad Rao, C.A. Leony Leon, K. Ueyama, M. Matsukata, Micropor. Mesopor. Mater. 21 (1998) 305.

[43] G. Giordano, A. Katovic, D. Caputo, Stud. Surf. Sci. Catal. 140 (2001) 307.